



Polyethylene interfacial dielectric layer for organic semiconductor single crystal based field-effect transistors

Min Chen^a, Boyu Peng^{a,*}, Xuyun Guo^b, Ye Zhu^b, Hanying Li^{a,*}

^a Department of Polymer Science and Engineering, MOE Key Laboratory of Macromolecular Synthesis and Functionalization, International Research Center for X Polymers, Shanxi-Zheda Institute of Advanced Materials and Chemical Engineering, Zhejiang University, Hangzhou 310027, China

^b Department of Applied Physics, Research Institute for Smart Energy, The Hong Kong Polytechnic University, Hong Kong 999077, China

ARTICLE INFO

Article history:

Received 12 June 2023

Revised 3 September 2023

Accepted 4 September 2023

Available online 9 September 2023

Keywords:

Polyethylene

Interfacial dielectric layer

Organic semiconductor

Single crystal

Organic field-effect transistors

ABSTRACT

Organic semiconductor single crystals (OSSCs) have shown their promising potential in high-performance organic field-effect transistors (OFETs). The interfacial dielectric layers are critical in these OFETs as they not only govern the key semiconductor/dielectric interface quality but also determine the growth of OSSCs by their wetting properties. However, reported interfacial dielectric layers either need rigorous preparation processes, rely on certain surface chemistry reactions, or exhibit poor solvent resistance, which limits their applications in low-cost, large-area, monolithic fabrication of OSSC-based OFETs. In this work, polyethylene (PE) thin films and lamellar single crystals are utilized as the interfacial dielectric layers, providing solvent resistive but wettable surfaces that facilitate the crystallization of 6,13-bis(triisopropylsilyl)ethynyl)pentacene (TIPS-PEN) and 6,13-bis(triisopropylsilyl)ethynyl)-5,7,12,14-tetraazapentacene (TIPS-TAP). As evidenced by the presence of ambipolar behavior in TIPS-PEN single crystals and the high electron mobility ($2.3 \pm 0.34 \text{ cm}^2 \text{ V}^{-1} \text{ s}^{-1}$) in TIPS-TAP single crystals, a general improvement on electron transport with PE interfacial dielectric layers is revealed, which likely associates with the chemically inertness of the saturated C-H bonds. With the advantages in both processing and device operation, the PE interfacial dielectric layer potentially offers a monolithic way for the enhancement of electron transport in solution-processed OSSC-based OFETs.

© 2024 Published by Elsevier B.V. on behalf of Chinese Chemical Society and Institute of Materia Medica, Chinese Academy of Medical Sciences.

Organic field-effect transistors (OFETs) are widely recognized as one of the potential semiconductor technologies, thanks to the advantages including flexible, low-cost, light-weight [1–5], *etc.* It is generally acknowledged that charge transport takes place near the interface between semiconductor and gate dielectric in OFETs [6,7]. Hence, the interface quality plays important role in determining the performance of OFETs, such as mobility [8], hysteresis [9], stability [10], subthreshold swing [11]. Efforts are first made to improve the interface quality from the semiconductor side. From this regard, the organic semiconductor single crystals (OSSCs) are promising candidates by their long-ordered and less defects feature [12–18]. Direct growth of OSSCs *via* solution method on the gate dielectric is one of the widely adopted strategies to construct a high-quality semiconductor/dielectric interface [12,19–21]. In these cases, surface modification of gate dielectric is usually needed to improve the wettability and/or passivate the structural/energetic defects of the dielectric [22]. One representative example is the

passivation of surface hydroxyl groups that generally prohibit the electron transport in n-type and ambipolar OFETs [23].

For the region of dielectric layers near the semiconductor/dielectric interface (interfacial dielectric layer), appropriate wettability is primarily required in solution processing methods. In addition, solvent resistance is a more fundamental prerequisite for any interfacial dielectric layers. Crosslinking the polymer thin films is one effective strategy, for example in divinyltetramethylsiloxane-bis(benzocyclobutene) derivative (BCB) [24] and poly(methyl methacrylate) (PMMA) [8,25]. But the high temperature and inert atmosphere needed in the curing process limits its adaptability in OFETs. The covalently bonded self-assembled monolayers (SAMs) also effectively serve as interfacial dielectric layers, albeit material scope (SiO_2 , Al_2O_3 , *etc.*) [26,27] is strictly limited. Alternatively, polyethylene (PE), as the most widely used and basic polymer, potentially serves as a good interfacial dielectric layer. It is composed of saturated $-\text{CH}_2-$ groups, which offers the ability to screening the electron trap [24,28,29]. Furthermore, PE usually shows strong resistance to solvent that could keep the interfacial dielectric layer stable during the subsequent solution fabrication process of OSSCs. However, troubled by the

* Corresponding authors.

E-mail addresses: pengboyu@zju.edu.cn (B. Peng), hanying_li@zju.edu.cn (H. Li).

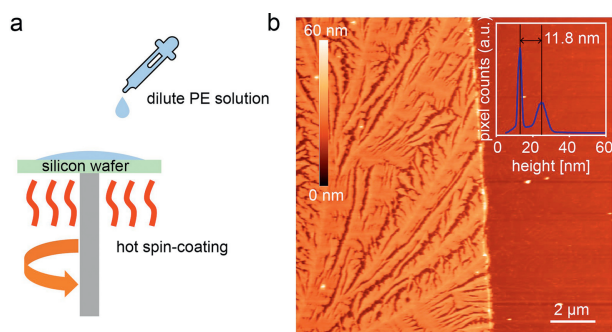


Fig. 1. (a) Schematic for the preparation process for the ultra-thin PE film. (b) Atomic force microscope (AFM) height image for the PE thin film (insertion: height statistic for the AFM image, exhibiting the thickness of PE thin film).

intrinsic strong crystallinity of PE, processing PE into thin and smooth films to be good interfacial dielectric layers has been a great challenge.

Here, ultra-thin PE films prepared *via* hot spin-coating are exploited as the interfacial dielectric layer on SiO₂. Single crystals of 6,13-bis(triisopropylsilylethynyl)pentacene (TIPS-PEN) and 6,13-bis(triisopropylsilylethynyl)-5,7,12,14-tetraazapentacene (TIPS-TAP) are deposited as the active layer in p-type and n-type OFETs, respectively. The TIPS-PEN based OFETs exhibit ambipolar transport, and TIPS-TAP based OFETs show an electron mobility as high as $2.3 \pm 0.34 \text{ cm}^2 \text{ V}^{-1} \text{ s}^{-1}$. Besides, considering that lamellar single crystal is the most uniform and ordered structure of PE, an attempt to apply PE lamellar single crystals (PELSCs) as interfacial dielectric layer in OFETs is carried out. PELSCs with lateral size up to 40 μm are obtained *via* self-seeding method. With PELSC/SiO₂ as gate dielectric and TIPS-PEN or TIPS-TAP single crystals as semiconductors, the OFETs shows hole and electron mobilities of $0.65 \pm 0.17 \text{ cm}^2 \text{ V}^{-1} \text{ s}^{-1}$ and $0.50 \pm 0.10 \text{ cm}^2 \text{ V}^{-1} \text{ s}^{-1}$, respectively. This work provides a facile strategy to optimize the quality of dielectric/semiconductor interface and demonstrate the superiority of nonpolar and hydrophobic PE in enhancing electron transport.

Ultra-thin PE films are prepared *via* hot spin-coating, with the schematic process shown in Fig. 1a and details in the experiment section (Supporting information). Morphology of the PE thin film is shown in Fig. 1b. In the PE thin film, branched single layer lamellae with average thickness of 11.8 nm are obtained. The thickness is similar to the characteristic thickness of polymer lamellar single

crystal, so that the lamellae are likely corresponding to the flat-on orientation [30–32].

The solvent resistance properties of the PE thin film are examined *via* immersing the PE thin film in common solvents for OSSCs growth under 50 °C. Six solvents are chosen for the examination, including chlorobenzene, chloroform, mesitylene, *m*-xylene, toluene and heptane. As shown in Figs. 2a–f, the structures of the PE thin films after immersing in six different solvents are similar to the pristine structure in Fig. 1b. The phenomenon demonstrates that the solvent treatment has negligible effect to the PE thin films. Furthermore, the ability of the PE thin film to facilitate the OSSC growth are studied with TIPS-PEN as example. *Via* the droplet-pinned crystallization (DPC) method [12,33], ribbon-like TIPS-PEN crystals are obtained from the six solvents mentioned above on the silicon wafer covered by the PE thin film. Although the PE thin film is slightly rougher than some representative interfacial dielectric layers, such as BCB, amorphous PMMA and SAMs, single crystalline feature of the TIPS-PEN crystals are still obtained as observed by the polarized optical microscopic (POM) images (bottom pictures in Figs. 2a–f), thanks to good wettability of solutions on the PE thin film and the air/liquid interface crystallization behavior of TIPS-PEN [25].

Electrical properties of OFETs with PE/SiO₂ as gate dielectric and TIPS-PEN single crystals as semiconductor are shown in Figs. 3a–c. Typical transport and output characterizations shown in Figs. 3d–g exhibit an ambipolar transport feature. For the hole transport, an average mobility of $0.29 \pm 0.10 \text{ cm}^2 \text{ V}^{-1} \text{ s}^{-1}$ (range: $0.10 \text{ cm}^2 \text{ V}^{-1} \text{ s}^{-1}$ to $0.47 \text{ cm}^2 \text{ V}^{-1} \text{ s}^{-1}$ for 12 devices) are obtained. And the threshold voltages (V_{TH}) are in the range between -55 V and -70 V. The current on-to-off ratios ($I_{\text{on}}/I_{\text{off}}$) are larger than 10^4 . For the electron transport, an average mobility of $0.0023 \pm 0.0018 \text{ cm}^2 \text{ V}^{-1} \text{ s}^{-1}$ (range: $0.00040 \text{ cm}^2 \text{ V}^{-1} \text{ s}^{-1}$ to $0.0063 \text{ cm}^2 \text{ V}^{-1} \text{ s}^{-1}$ for 12 devices) are obtained. And the threshold voltages are in the range between 60 V and 75 V. The $I_{\text{on}}/I_{\text{off}}$ are larger than 10^2 . Ambipolar transport feature of TIPS-PEN has been discovered in the conditions of using nonpolar solvents and screening the hydroxyl groups *via* polymer interfacial dielectric layers, such as BCB [34], PMMA [35]. Here, the ambipolar transport feature of TIPS-PEN based OFETs demonstrates the ability of the PE thin film to passivate the electron trap on the surface of SiO₂, thanks to the inert -CH₂- chemical structure and hydroxyl-free feature of PE.

To further examine the superiority of the PE thin film in passivating or screening the electron trap on dielectric interface and then facilitating the electron transport, n-type OFETs are constructed with PE/SiO₂ as gate dielectric and TIPS-TAP single crys-

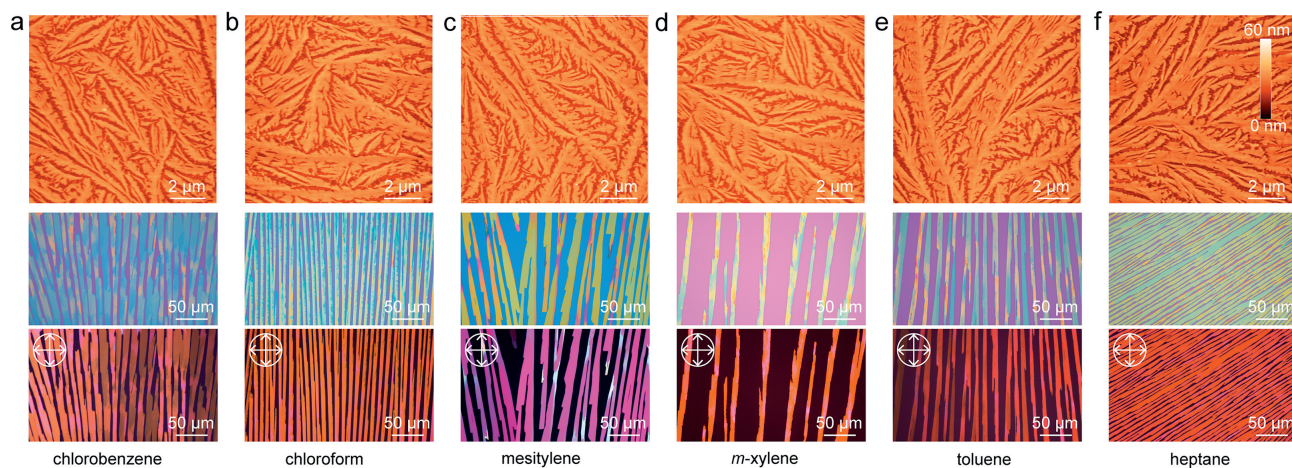


Fig. 2. The top figures are the AFM height images for PE thin films after immersing in solvents at 50 °C for 1 h, and the middle and the bottom figures are the optical microscopic (OM) and POM images for TIPS-PEN single crystals grown from different solvents: (a) chlorobenzene, (b) chloroform, (c) mesitylene, (d) *m*-xylene, (e) toluene, (f) heptane, respectively.

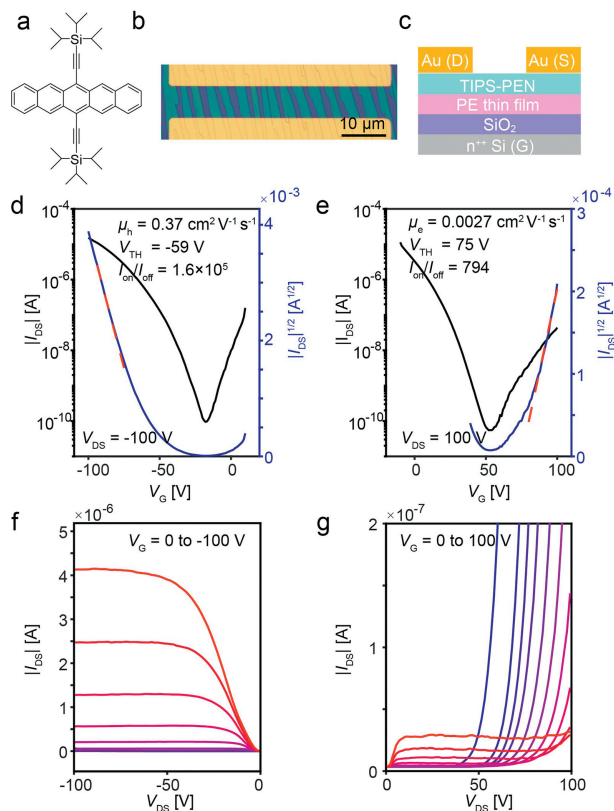


Fig. 3. (a) Molecule structure for TIPS-PEN. (b) OM image for the OFET device with TIPS-PEN single crystals as semiconductor. (c) Schematic diagram for the OFET device based on PE thin film. (d, f) Typical transfer and output characteristics for the OFETs under p-channel operation modes. (e, g) Typical transfer and output characteristics for the OFETs under n-channel operation modes.

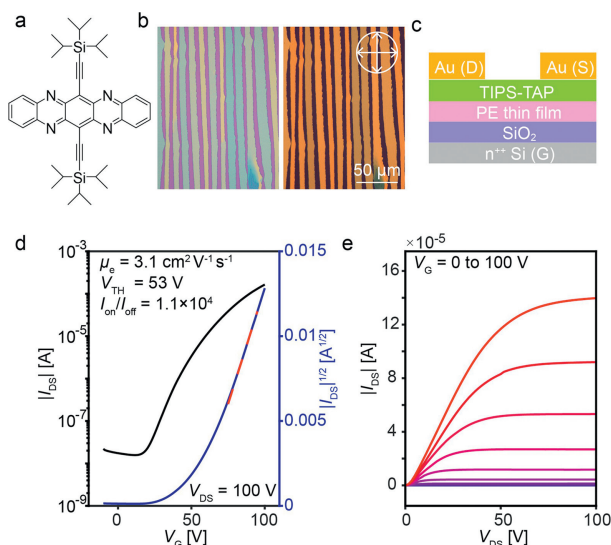


Fig. 4. (a) Molecule structure of TIPS-TAP. (b) OM and POM images for TIPS-TAP single crystals grown on PE thin film. (c) Schematic diagram for the OFET device based on PE thin film. (d, e) Typical transfer and output characteristics for the OFET.

tals as the semiconductor (Figs. 4a–c). As shown in Fig. 4b, ribbon-like TIPS-TAP single crystals are also obtained on the PE thin film. Typical transport and output characterizations of the n-type OFET are shown in Figs. 4d and e. Electron mobility of the OFETs shows an average value of $2.3 \pm 0.34 \text{ cm}^2 \text{ V}^{-1} \text{ s}^{-1}$ (range: $1.8 \text{ cm}^2 \text{ V}^{-1} \text{ s}^{-1}$ to $3.1 \text{ cm}^2 \text{ V}^{-1} \text{ s}^{-1}$ for 12 devices). The $I_{\text{on}}/I_{\text{off}}$ are larger than 10^3 and the V_{TH} are in the range between 40V and 60V. Although

the PE thin film shows a relative high surface roughness, electron mobility of the OFETs modified by PE thin film are similar to the reported TIPS-TAP single crystals based OFETs with smooth gate dielectric modified by octadecylphosphonic acid [36], 12-cyclohexyldodecylphosphonic acid [37], and BCB [38]. The phenomenon might be attributed to the high-quality TIPS-TAP single crystals which grow at the solution/air interface and then fall to the PE thin film substrate [25]. The roughness of the substrate thus shows minor impact on the crystal growth.

As discussed above, the PE thin film shows superiority in modifying the dielectric surface, including adapting solution wettability of substrate and passivating electron trap of dielectric. Further optimizing the surface properties of PE thin film such as surface roughness, degree of order is expected. Lamellar single crystal, as the most ordered structure of semicrystalline polymers, can be an ideal candidate for the gate dielectric of OFETs. Hence, PE lamellar single crystals (PELSCs) are prepared and applied in OFETs as interfacial dielectric layer on SiO_2 .

PELSCs are grown in dilute solution via self-seeding method. As shown in Fig. 5a, the PELSC shows a hexagonal lateral shape with lateral size of about $40 \mu\text{m}$. The selected area electron diffraction (SAED) patterns shows that the PELSC corresponding to an orthorhombic crystal form with c-axis perpendicular to the crystal surface (Fig. 5b). Thickness of the PELSC is examined by AFM. Statistic of the AFM height image exhibits that the thickness of PELSC is 12.37 nm (Fig. 5c). The PELSC shows a uniform thickness and smooth surface without spiral dislocation or sub-microscopic defects. The outstanding surface quality makes the PELSC, compared with its thin film counterparts, a more promising candidate to improve the quality of gate dielectric/semiconductor interface in OFETs.

OFETs with PELSC/ SiO_2 as gate dielectric and TIPS-PEN or TIPS-TAP single crystals as semiconductors are obtained (Figs. 6a and b). TIPS-PEN and TIPS-TAP single crystals are directly grown on silicon wafer locally covered with PELSC. Devices are constructed in the overlapping area of PELSC and ribbon-like semiconductor single crystals.

Electrical performances of the OFETs are shown in Figs. 6c–f. For the TIPS-PEN single crystals based OFETs, an average hole mobility of $0.65 \pm 0.17 \text{ cm}^2 \text{ V}^{-1} \text{ s}^{-1}$ (range: $0.33 \text{ cm}^2 \text{ V}^{-1} \text{ s}^{-1}$ to $0.81 \text{ cm}^2 \text{ V}^{-1} \text{ s}^{-1}$ for 5 devices), $I_{\text{on}}/I_{\text{off}} > 10^3$, V_{TH} in the range between -30 V and -65 V are obtained. For the TIPS-TAP single crystals based OFETs, an average electron mobility of $0.50 \pm 0.10 \text{ cm}^2 \text{ V}^{-1} \text{ s}^{-1}$ (range: $0.38 \text{ cm}^2 \text{ V}^{-1} \text{ s}^{-1}$ to $0.62 \text{ cm}^2 \text{ V}^{-1} \text{ s}^{-1}$ for 5 devices), $I_{\text{on}}/I_{\text{off}} > 10^3$, V_{TH} in the range between 35 V and 60 V are obtained. Different from the above expectation, compared to PE thin film/ SiO_2 gate dielectric, ambipolar transport of TIPS-PEN is not shown on the PELSC/ SiO_2 gate dielectric, and the electron mobility of TIPS-TAP shows a slight decrease. The phenomenon might be attributed to the relatively poor quality of the TIPS-PEN and TIPS-TAP single crystals. During the growth process of TIPS-PEN or TIPS-TAP single crystals, the uncovered SiO_2 region and the PELSC region shows different wettability to the semiconductor solution. And the continuous growth of semiconductor single crystal would be disturbed when they grow from the SiO_2 region to PELSC region. Hence, only few continuous TIPS-PEN or TIPS-TAP single crystals could be found on PELSC. The disturbance of crystal growth might lead to poor crystal quality and then result in the decrease of the electrical performance. Although the limited size of the PELSC do not fully manifest its application potential in OFETs, we believe this could shortly be overcome by improving the fabrication technique.

In summary, PE is employed as the interfacial dielectric layer in OFETs. Thanks to the outstanding solvent resistance and wettability, single crystals of semiconductors including TIPS-PEN and TIPS-TAP could be obtained either on PE thin films or PELSCs. Based on the PE thin film, OFETs with TIPS-PEN single crystals as semicon-

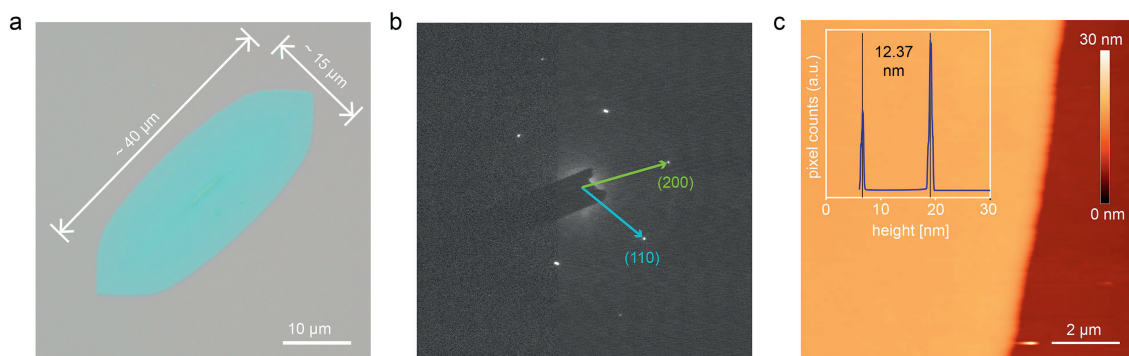


Fig. 5. (a) OM image of PELSC. (b) SAED patterns for PELSC. (c) AFM height image for PELSC (insertion: height statistic for the AFM image, exhibiting the thickness of PELSC).

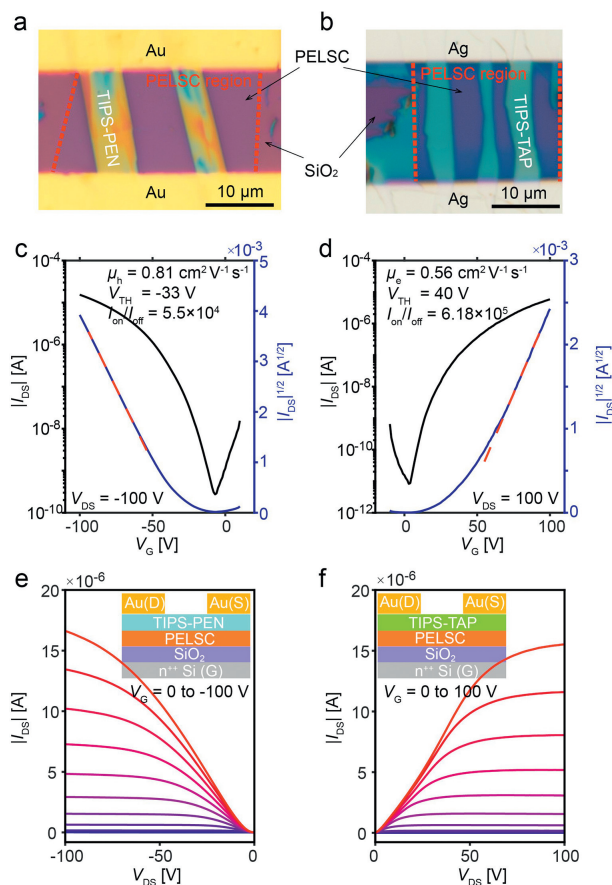


Fig. 6. (a, b) OM images for the channel in OFETs based on PELSCs with TIPS-PEN and TIPS-TAP single crystals as semiconductor, respectively. (c, e) Typical transfer and output characteristics for the OFETs with TIPS-PEN single crystals as semiconductor. (d, f) Typical transfer and output characteristics for the OFETs with TIPS-TAP single crystals as semiconductor.

ductor exhibit ambipolar transport and OFETs with TIPS-TAP single crystals as semiconductor show an electronic mobility as high as $2.3 \pm 0.34 \text{ cm}^2 \text{ V}^{-1} \text{ s}^{-1}$. The capability of PE thin film to facilitate electron transport could be ascribed to its hydrophobic feature and the ability to screen the electron trap on SiO_2 dielectric. Parallely, the lamellar single crystals that offer the most orderly packed PE polymer chains are obtained. OFETs with PELSC/ SiO_2 as gate dielectric and TIPS-PEN and TIPS-TAP single crystals as semiconductors show a hole mobility of $0.65 \pm 0.17 \text{ cm}^2 \text{ V}^{-1} \text{ s}^{-1}$ and an electron mobility of $0.50 \pm 0.10 \text{ cm}^2 \text{ V}^{-1} \text{ s}^{-1}$, respectively. Unlike the cross-linked polymers or SAMs that rely specific chemical reactions to

serve as the interfacial dielectric layers, this works provides a pure physical strategy to use PE thin films and crystals as the interfacial dielectric layers in OFETs. In addition to the solvent wettability, solvent resistance and the capability to screen surface traps, such a physical strategy has advantages in monolithic preparation that can broaden the selection of dielectric materials, which is meaningful to the development of OFETs.

Declaration of competing interest

The authors declare that they have no known competing financial interests or personal relationships that could have appeared to influence the work reported in this paper.

Acknowledgments

This work was supported by the National Key Research and Development Program of China (Nos. 2019YFE0116700, 2019YFA0705900) funded by MOST, National Natural Science Foundation of China (Nos. 51873182, 52103231), Zhejiang Province Science and Technology Plan (No. 2021C04012) funded by Zhejiang Provincial Department of Science and Technology, and Shanxi-Zheda Institute of Advanced Materials and Chemical Engineering (No. 2021SZ-FR003). The authors acknowledge the support by the Fundamental Research Funds for the Central Universities (No. 226-2023-00113).

Supplementary materials

Supplementary material associated with this article can be found, in the online version, at doi:10.1016/j.ccl.2023.109051.

References

- [1] Y. Yan, Y. Zhao, Y. Liu, J. Polym. Sci. 60 (2022) 311–327.
- [2] S. Yuvaraja, A. Nawaz, Q. Liu, et al., Chem. Soc. Rev. 49 (2020) 3423–3460.
- [3] G. Zhang, C. Xie, P. You, S. Li, Organic field-effect transistors, in: G. Zhang, C. Xie, P. You, S. Li (Eds.), Introduction to Organic Electronic Devices, Springer Nature Singapore, Singapore, 2022, pp. 107–129.
- [4] Y. Zhao, W. Wang, Z. He, et al., Chin. Chem. Lett. 34 (2023) 108094.
- [5] H. Siringhaus, Adv. Mater. 26 (2014) 1319–1335.
- [6] H. Chen, W. Zhang, M. Li, G. He, X. Guo, Chem. Rev. 120 (2020) 2879–2949.
- [7] C. Di, Y. Liu, G. Yu, D. Zhu, Acc. Chem. Res. 42 (2009) 1573–1583.
- [8] Y. Wang, X. Huang, T. Li, et al., Chem. Mater. 31 (2019) 2212–2240.
- [9] T.D. Tsai, J.W. Chang, T.C. Wen, T.F. Guo, Adv. Funct. Mater. 23 (2013) 4206–4214.
- [10] Z. Wang, H. Lin, X. Zhang, et al., Sci. Adv. 7 (2021) eabf8555.
- [11] F. Yang, L. Jin, L. Sun, et al., Adv. Mater. 30 (2018) 1801891.
- [12] B. Peng, R. Wu, H. Li, Acc. Chem. Res. 54 (2021) 4498–4507.
- [13] J. Qian, S. Jiang, S. Li, et al., Adv. Mater. Technol. 4 (2019) 1800182.
- [14] R. Wu, B. Peng, H. Li, H. Li, Chem. Mater. 33 (2021) 19–38.
- [15] L. Zhang, M. Mehedi Hasan, Y. Tang, et al., Mater. Today 50 (2021) 442–475.
- [16] X. Zhang, W. Deng, R. Jia, X. Zhang, J. Jie, Small 15 (2019) 1900332.
- [17] X. Zhang, H. Dong, W. Hu, Adv. Mater. 30 (2018) 1801048.
- [18] X. Zhao, H. Zhang, J. Zhang, et al., Adv. Sci. 10 (2023) 2300483.

- [19] Y. Diao, B.C.K. Tee, G. Giri, et al., *Nat. Mater.* 12 (2013) 665–671.
- [20] W. Zhao, J. Jie, Q. Wei, et al., *Adv. Funct. Mater.* 29 (2019) 1902494.
- [21] S. Chen, Z. Li, Y. Qiao, Y. Song, *J. Mater. Chem. C* 9 (2021) 1126–1149.
- [22] B. Fu, F. Yang, L. Sun, et al., *Adv. Mater.* 34 (2022) 2203330.
- [23] J. Zaumseil, H. Sirringhaus, *Chem. Rev.* 107 (2007) 1296–1323.
- [24] L.L. Chua, J. Zaumseil, J.F. Chang, et al., *Nature* 434 (2005) 194–199.
- [25] H. Li, J. Wu, K. Takahashi, et al., *J. Am. Chem. Soc.* 141 (2019) 10007–10015.
- [26] J.W. Borchert, U. Zschieschang, F. Letzkus, et al., *Sci. Adv.* 6 (2020) eaaz5156.
- [27] H. Klauk, U. Zschieschang, J. Pflaum, M. Halik, *Nature* 445 (2007) 745–748.
- [28] A.D. Scaccabarozzi, J.I. Basham, L. Yu, et al., *J. Mater. Chem. C* 8 (2020) 15406–15415.
- [29] Y. Kanbur, M. Irimia-Vladu, E.D. Głowacki, et al., *Org. Electron.* 13 (2012) 919–924.
- [30] Y. Wang, M. Rafailovich, J. Sokolov, et al., *Phys. Rev. Lett.* 96 (2006) 028303.
- [31] Y. Wang, S. Ge, M. Rafailovich, et al., *Macromolecules* 37 (2004) 3319–3327.
- [32] E. Woo, M. Park, Y.G. Jeong, K. Shin, *J. Appl. Polym. Sci.* 123 (2012) 2558–2565.
- [33] H. Li, B.C.K. Tee, J.J. Cha, et al., *J. Am. Chem. Soc.* 134 (2012) 2760–2765.
- [34] G. Xue, C. Fan, J. Wu, et al., *Mater. Horiz.* 2 (2015) 344–349.
- [35] C. Lin, B. Peng, J. Wu, et al., *Adv. Electron. Mater.* 8 (2022) 2200557.
- [36] D. Liu, X. Xu, Y. Su, et al., *Angew. Chem. Int. Ed.* 52 (2013) 6222–6227.
- [37] D. Liu, Z. He, Y. Su, et al., *Adv. Mater.* 26 (2014) 7190–7196.
- [38] G. Xue, J. Wu, C. Fan, et al., *Mater. Horiz.* 3 (2016) 119–123.